

Extended Infrared Emission from (U)LIRGs

Vassilis Charmandaris^{1,2,3}

¹*Dept. of Physics & ITCP, University of Crete, GR-71003, Heraklion, Greece*

²*IESL/FORTH, GR-71110, Heraklion, Greece*

³*Chercheur Associé, Observatoire de Paris, F-75014, Paris, France*

Abstract.

I discuss recent findings on the presence the extended emission of a volume limited ($d < 82$ Mpc) sample of luminous infrared galaxies(LIRGs) drawn from the Great Observatories All-sky LIRG Survey (GOALS) galaxy sample. Using Spitzer/IRS spectra to determine the fraction of emission arising from their extended component, we find the majority of LIRGs, at least $\sim 20\%$ (and up to $\sim 80\%$) of their emission stems from an extended component. The IRS spectra also allow us to separate the different emission components (dust continuum and PAH feature emission, ionized and molecular gas) and calculate their corresponding spatial extent. We find that in several galaxies the PAH feature emission is more extended (up to 3 times) than that of the mid-infrared continuum. These results suggest that mid-infrared emission of LIRGs is not as compact as in their more luminous counterparts (ULIRGs) but instead it is distributed across their disks. Ongoing analysis of the extent of the different components will also enable us to ascertain whether the high redshift, higher luminosity submillimeter galaxies (SMGs), which also display fairly extended star formation, can be considered the scaled-up luminosity examples of local LIRGs, rather than ULIRGs.

1. Introduction

The discovery by the Infrared Astronomical Satellite (IRAS) of luminous and ultra-luminous infrared (IR) galaxies, the so called LIRGs and ULIRGs¹, has opened a new window in extragalactic astrophysics. Over the past 25 years, follow up ground-based and space-born observations of these optically faint systems (see Houck et al. 1984) have revealed much about their detailed physical properties as well as their contribution to the integrated energy production in the Universe (see Sanders & Mirabel 1996, and references therein). More specifically it has been shown that even though LIRGs and ULIRGs are not very common in the local Universe (Soifer & Neugebauer 1991), they contribute a substantial fraction of the energy at $z \sim 1 - 2$ (Pérez-González et al. 2005; Le Floch et al. 2005; Caputi et al. 2007). Furthermore, the more IR luminous systems tend to be more disturbed dynamically, show evidence of merging, and often harbor an active galactic nucleus (AGN). The leap in sensitivity provided by the *Spitzer*

¹LIRGs are defined as systems displaying an infrared luminosity, L_{IR} , of: $10^{11} L_{\odot} \leq L_{\text{IR}[8-1000\mu\text{m}]} < 10^{12} L_{\odot}$; ULIRGs: $L_{\text{IR}[8-1000\mu\text{m}]} \geq 10^{12} L_{\odot}$.

Space Telescope (Werner et al. 2004) and in particular the availability of deep mid-infrared (MIR) spectroscopy with the Infrared Spectrograph (IRS; Houck et al. 2004) enabled the detailed study of the properties of large nearby (i.e., Armus et al. 2007, Desai et al. 2007, Imanishi et al. 2008, Farrah et al. 2008; Pereira-Santaella et al. 2010) and more distant (Houck et al. 2005; Yan et al. 2005) samples of (U)LIRGs. It thus became evident that, given the diversity of the MIR spectra of LIRGs and even more of ULIRGs, these systems cannot be grouped in a common class of galaxies either in terms of their MIR and/or far-infrared (FIR) properties. A number of correlations between the MIR colors, strength of features due to polycyclic aromatic hydrocarbons (PAHs), and line emissions, with the dominant source of energy production or interaction stage of galaxies have been explored (Armus et al. 2007; Desai et al. 2007; Veilleux et al. 2009, Petric et al. 2011). It appears that systems which are AGN dominated show weak PAH features, which are also correlated with the FIR spectral slope. Systems with greater MIR luminosity display weaker PAH emission, while dust extinction, quantified by the $9.7\mu\text{m}$ silicate feature, varies in strength and does not correlate with starburst or AGN dominated systems.

Recently, some studies have suggested that $z \sim 2$ ULIRGs are not just the analogs of local ULIRGs but instead they display MIR spectral features more similar to those seen in local, lower luminosity starburst galaxies and LIRGs (Farrah et al. 2008; Rigby et al. 2008). Some high- z sub-millimeter galaxies (SMGs) with IR luminosities similar to or greater than ULIRGs also show IR properties different from local ULIRGs (Pope et al. 2008; Murphy et al. 2009; Menéndez-Delmestre et al. 2009). All this evidence, in combination with results obtained from spatially resolved $\text{H}\alpha$ imaging and CO and radio maps of SMGs, suggest that the star formation (SF) taking place in ULIRGs and some SMGs at high redshift may be occurring over large areas, extending over several kpc across their disks (Bothwell et al. 2010; Ivison et al. 2010; Alexander et al. 2010). This is in contrast to what is seen in local ULIRGs where the strong bursts of SF are concentrated within the central kpc of galaxies probably due to interactions and mergers (Sanders & Mirabel 1996, Downes & Solomon 1998; Bryant & Scoville 1999; Soifer et al. 2000), which efficiently drive gas and dust towards their nuclei.

In the present paper I present a summary of the recent results obtained on the issue of extended emission in the $5\text{-}15\mu\text{m}$ range using the Infrared Spectrograph on Spitzer. More detailed analysis is available in Díaz-Santos et al. (2010b, 2011).

1.1. Observations and Analysis

The sample on which we base our analysis is the Great Observatories All-Sky LIRG Survey (GOALS; Armus et al. 2009). GOALS comprises a complete, flux-limited sample of galaxies in the local Universe drawn from the Revised Bright Galaxy Sample (RBGS, Sanders et al. 2003) selected to be systems in the (U)LIRG luminosity class. Armus et al. (2009) describe in detail how the sample was selected as well the global characteristics. Additional information related to the presence on an active galactic nucleus (AGN) is discussed by Petric et al. (2011). More specifically using a number of MIR diagnostics, Petric et al. (2011) estimate the AGN contribution to the MIR luminosity of the systems and, based on their apparent morphology, classify each galaxy into a stage of interaction, ranging from isolated systems to advanced mergers. In Howell et al. (2010) the relation between the UV and MIR emission of the galaxies in the sample is investigated while Haan et al. (2011) present a thorough analysis of the nuclear structure of the sample using high spatial resolution NIR and optical images with

Hubble Space Telescope. We refer the reader to these papers since we will rely on their findings in the interpretation of our results. Out of the 291 galaxies (202 systems) included in the GOALS sample (see Armus et al. 2009), a total of 221 are used for this study. A table with their main physical characteristics such as the distance, L_{IR} , or FIR colors can be found in Díaz-Santos et al. (2010b).

Our analysis focuses on the calculation of the fraction of extended emission of galaxies as a function of wavelength, FEE_{λ} , which is defined as the fraction of emission in a galaxy that does *not* arise from a spatially unresolved central component. Detailed information on the calculation of the FEE_{λ} functions can be found on Díaz-Santos et al. (2010b). For practical purposes, we remind the reader that its formal definition is:

$$FEE_{\lambda} = \frac{EE_{\lambda}}{E_{\lambda}(\text{total})} \quad (1)$$

where FEE_{λ} , EE_{λ} and $E_{\lambda}(\text{total})$ are the fraction extended emission (ranging from zero to unity), the extended emission, and the total emission of a galaxy at each wavelength respectively. We also define the core size of a galaxy as the full width half-maximum (FWHM) of a Gaussian fitted to the spatial profile of its nuclear emission along the Spitzer/IRS slit at a given wavelength. Note that while the core size represents how extended the nuclear emission is, the FEE also accounts for low surface brightness emission more extended than the core of the source, that is found beyond the wings of the central Gaussian.

2. Results

The fraction of the extended emission as a function of wavelength, FEE_{λ} , calculated for each one of the sources, contains a wealth of information. In the present section we discuss the types of FEE_{λ} we typically see in our sample, as well as the properties of the extended emission in the MIR continuum. For the latter we use as reference the resolution element at $13.2\ \mu\text{m}$ ($FEE_{13.2\mu\text{m}}$), as it is an area of the spectrum which is devoid of known emission or absorption features. Our findings though are similar for the $5 - 15\ \mu\text{m}$ MIR continuum in general. A detailed comparison of the FEE_{λ} for different MIR spectral features (e.g., PAHs, emission lines or the $9.7\ \mu\text{m}$ silicate absorption feature) and the correlation of their ratios with the characteristics of each galaxy (e.g., nuclear and total extinction, presence of an AGN) is addressed in a companion paper (Díaz-Santos et al. 2011). In addition, we construct spectra for the nuclear and extended components of galaxies as a function of the FEE_{λ} types.

2.1. Types of FEE_{λ} Profiles

If one ignores projection effects or details on the intrinsic geometry of a source, the spatial profile of a galaxy as a function of wavelength, and consequently the estimated FEE_{λ} , depends primarily on the origin of the emission within the galaxy. The MIR continuum emission, PAH features, emission lines, as well as absorption features do not always originate from the same physical regions. Therefore it is reasonable to expect that the FEE_{λ} function varies among the galaxies. We find three different FEE_{λ} types, whose shapes are similar among the galaxies examined here. We exclude from this study 8 sources (4% of the sample) that appear practically unresolved in the $5 - 15\ \mu\text{m}$ range and for which their $FEE_{\lambda} \simeq 0$. We also exclude 11 galaxies (5% of the sample) whose FEE_{λ} could not be classified in any of the three types.

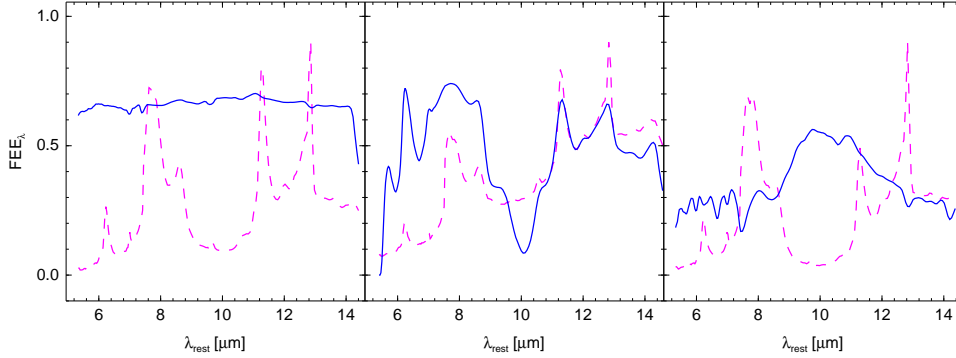


Figure 1. FEE_λ function of 3 galaxies that serve as examples of the 3 types identified in the sample (blue solid line). The spectrum of each galaxy, scaled to arbitrary units, is also plotted for reference (pink dashed line). The galaxies are: NGC 3110 (left), NGC 1365 (center), and MCG+08-11-002 (right). The FEE_λ functions have been smoothed with a 4-pixel box to reduce the noise. Left panel: Constant/featureless FEE_λ . Middle panel: PAH and line extended emission. Right panel: Silicate-extended emission.

- Constant/featureless: 111 (50%) (U)LIRGs display a constant FEE_λ across the whole IRS 5–15 μm wavelength range (see Figure 1, left panel). No MIR feature appears more extended than another or even than the continuum emission. This implies that there is no differentiation in the spatial distribution of the type of emitting region along the IRS slit. These constant FEE_λ functions range between ~ 0.1 up to ~ 0.85 among the galaxies of this type. A representative member of this type is NGC 3110 that, in particular, have a constant FEE_λ of ~ 0.65 .
- PAH- and line-extended: 37 galaxies (17%) of the sample show MIR features which are clearly more extended than the continuum emission (see Figure 1, central panel). More than $\sim 20\%$ of the flux detected in several PAH features and emission lines is extended, and in some sources it can be as high as 70%. In these type of galaxies, the bulk of the continuum emission originates from a circumnuclear region more compact than that giving rise to the MIR spectral features. The fact that these two components of emission are spatially decoupled suggests that, contrary to the previous type of FEE_λ , different physical processes are responsible for the energy production in the nucleus and in the disk. This could be due to the presence of either an AGN or intense starburst in the nucleus producing a strong MIR continuum, compared to a more quiescent, star formation on the disk where older stellar populations may heat the gas and PAH molecules. A representative member of this type is NGC 1365.
- Silicate-extended: Another 54 (24%) galaxies of the sample show a rather interesting FEE_λ shape in which the maximum peaks around 10 μm (see Figure 1, right panel). Inspecting the FEE_λ more closely, it appears that there is an increase between ~ 8 and 12 μm , around the wavelength range where the 9.7 μm silicate absorption feature is present. We attribute this maximum to an extinction effect in these systems. Galaxies containing very obscured nuclei will show little or not at all “unresolved emission”, at wavelengths dominated by the silicate absorption feature. As mentioned earlier, we always normalize the spatial profile of an unresolved point source to the source profile at every wavelength and subtract it in order to determine the value of FEE_λ . Consequently, if the nucleus

of a galaxy is very extinguished, any residual emission within the $9.7\mu\text{m}$ band, when compared to the emission at any other wavelength that is not affected by the absorption feature, would be interpreted as an excess in the fraction of extended emission originating from the outer disk of these galaxies, where the extinction is less extreme. This is reflected in the form of FEE_λ we compute, and implies that the silicate strength (i.e., the apparent optical depth) calculated from the integrated spectrum of these galaxies may not be representative of their nuclei (see Spoon et al. 2004). A representative member of this type is MCG+08-11-002.

The presence of these types of FEE_λ , suggest that the mechanism by which local (U)LIRGs produce the MIR emission in their disks and nuclear regions varies from one source to the next. There is a great diversity not only in the integrated spectrum of a LIRG/ULIRG, but also in the spatial distribution of the regions responsible for the formation of the various MIR features, such as PAHs, emission lines, and dust continuum. The FEE_λ measured indicates that in some galaxies the emission from PAHs, atomic or molecular lines is more extended than the dust continuum emission, while in others their extent is similar. These variations are clearly related to the location and intensity of the physical process producing the emission detected, such as young star clusters or an AGN. Our results suggest that not all local (U)LIRGs are to be a priori considered as compact, uniform MIR emitters. There has been an interesting such case reported already, VV114, a system with $L_{\text{IR}} = 4 \times 10^{11} L_\odot$ harboring an AGN, for which high resolution ground-based MIR imaging (Soifer et al. 2001), as well as $5 - 15\mu\text{m}$ ISO/CAM spectral maps reveal that nearly 60% of the MIR emission is extended (Le Flocc'h et al. 2002). This is understood since in these systems the MIR emission is not necessarily dominated by an AGN or a single burst of star formation. Moreover, in the cases of purely starburst-driven (U)LIRGs, the PAH and continuum emission may not be associated to the same star formation event but instead are probably excited, as a whole, by different stellar populations. For example the $11.3\mu\text{m}$ PAH emission is more representative of *recent* star formation event with ages greater than $8 - 10$ Myr, while *current* star formation, less than $8 - 10$ Myr in age, is better traced by the [NeII] $12.81\mu\text{m}$ or MIR continuum emission (Díaz-Santos et al. 2010a). In these galaxies, older star formation traced by PAH emission is more extended and is more typical of galactic disks, while recent star formation, associated to MIR continuum emission, is more compact and concentrated towards the nucleus.

2.2. The L_{IR} Dependence of the Extended Emission

We have calculated the median FEE_λ over the whole $5 - 15\mu\text{m}$ range, for all the galaxies in our sample and find that 32% of the galaxies have a median FEE_λ larger than 0.5, that is, at least 50% of the MIR emission of these galaxies is extended. In addition, more than 90% of the galaxies have a median FEE_λ larger than 0.1.

High resolution MIR images of a handful of local (U)LIRGs have revealed rather compact emission originating from a few hundred parsecs around their nuclei (Soifer et al. 2000, 2001; Díaz-Santos et al. 2008). This trend is also present in our data, even though the physical scales we probe with *Spitzer* are larger. In Figure 3 of Díaz-Santos et al. (2010b) we show three histograms of the median FEE_λ for galaxies grouped in three ranges of IR luminosity. We note that galaxies with the $L_{\text{IR}} < 10^{11.25} L_\odot$ and $10^{11.25} L_\odot \leq L_{\text{IR}} < 10^{12} L_\odot$ display similar median values of their FEE_λ distributions. The median of each histogram is 0.46 and 0.39 respectively, which is in agreement with previous studies based on smaller samples of LIRGs (Pereira-Santaella et al. 2010).

The median values of the low IR luminosity bins are very similar to that found for the median FEE_λ distribution of the whole sample of galaxies, 0.40. However, we find that the median of the corresponding distribution for ULIRGs (blue histogram) is only 0.14. A Kolmogorov-Smirnov (K-S) test comparing the two LIRG samples with that of the ULIRG indicates significance levels lower than 1×10^{-5} , implying that it is very unlikely that ULIRGs are drawn from the same parent distribution as LIRGs. Our data therefore suggest that, as a whole, the median FEE_λ of ULIRGs is 2 – 3 times lower than that of LIRGs.

In Figure 2a we display the spectra of the different FEE_λ types for the unresolved and extended components together. We note that the spectral features of the extended component are very similar in all FEE_λ types. Therefore the global properties of the physical mechanism responsible for this emission, that is the star formation in the external parts (disks) of galaxies ($d \gtrsim 2$ kpc) are the same. On the opposite, the spectra of the unresolved component are substantially different among the three FEE_λ types even though the $f_{13.2\mu\text{m}}/f_{5.5\mu\text{m}}$ continuum ratio is surprisingly similar in all of them, ranging between $\sim 9 - 11$. The difference between the MIR spectra of the unresolved emission of the constant and silicate-dominated FEE_λ types can be explained in terms of dust obscuration, with the silicate-dominated FEE_λ type having a larger $9.7 \mu\text{m}$ optical depth. The relative emission of the PAHs with respect to that of the continuum in the unresolved spectrum of the PAH-dominated FEE_λ type is lower than in the constant/featureless FEE_λ type, implying that some mechanism is either destroying the PAH carriers in the nuclei of these galaxies, or simply diluting their strength (peak to continuum ratio) by heating the dust grain to higher temperatures thus increasing the MIR continuum emission.

We now explore whether the spatial extent of the MIR continuum of (U)LIRGs is a smooth function of their IR luminosity, or whether there is a certain L_{IR} above which their properties change drastically making their emission substantially more concentrated. The blue circles in Figure 2b show the FEE of the $13.2 \mu\text{m}$ continuum emission ($FEE_{13.2\mu\text{m}}$) as a function of the L_{IR} for the galaxies in our sample. The size of the circles scales with their distance. As we can see, LIRGs display a wide range of $FEE_{13.2\mu\text{m}}$. They vary from compact systems ($FEE_{13.2\mu\text{m}} \simeq 0$) to others which are very extended ($FEE_{13.2\mu\text{m}} \simeq 0.85$). No clear trend with L_{IR} is evident over the decade in IR luminosity covered by the LIRGs. However, if we examine the median value of the $FEE_{13.2\mu\text{m}}$ calculated in different luminosity bins (black line), this appears to decrease as the L_{IR} of the galaxies increases, going from $\simeq 0.5$ at $L_{\text{IR}} \simeq 10^{10.3} L_\odot$ to $\simeq 0.1$ at $L_{\text{IR}} \simeq 10^{12.3} L_\odot$. Moreover, for IR luminosities above $\sim 10^{11.8} L_\odot$, just below the nominal transition between LIRGs and ULIRGs, the maximum of the $FEE_{13.2\mu\text{m}}$ (upper dashed line) drops abruptly, and only a few galaxies have $FEE_{13.2\mu\text{m}}$ values larger than 0.2. Indeed, all ULIRGs are unresolved and have $FEE_{13.2\mu\text{m}} \lesssim 0.2$.

One may consider that the decrease of the median $FEE_{13.2\mu\text{m}}$ with L_{IR} is due to the loss of spatial resolution. However as we discuss in detail in Díaz-Santos et al. (2010b) despite the limited resolution of Spitzer/IRS compared to ground-based facilities this does not affect our conclusions. It appears that there is a real threshold in the distribution of the compactness of IR bright galaxies happening at $L_{\text{IR}} \sim 10^{11.8} L_\odot$, with higher luminosity systems being more compact. Taking into account the lower and/or upper limits our data we find that the mean core size of LIRGs at $13.2 \mu\text{m}$ is 2.6 ± 0.1 kpc. Regarding the ULIRG sub-sample, establishing a typical size for the region from which their extended emission originates is even more challenging since all of them are un-

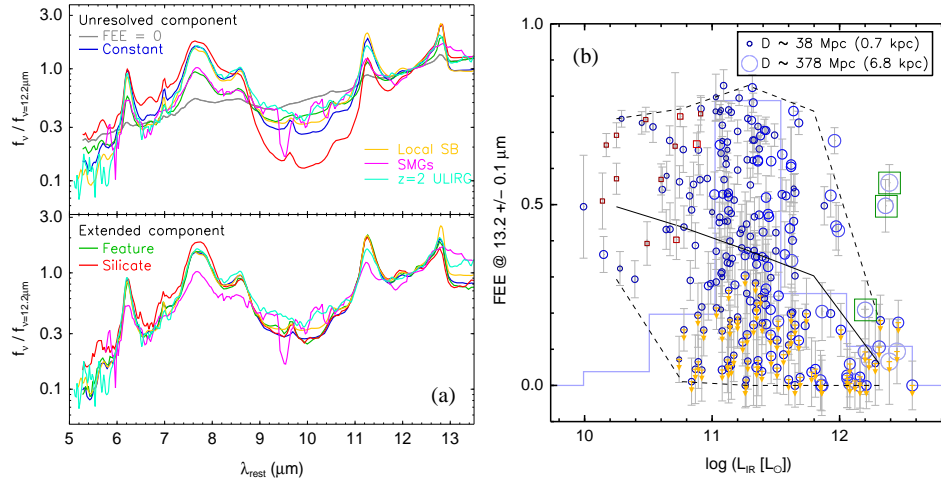


Figure 2. a) Averaged spectra of the different FEE_{λ} types scaled to $12.2 \mu\text{m}$ (unresolved: grey; constant/featureless: blue; PAH-dominated: green; silicate-dominated: red). The nuclear and extended emission components of each type are presented in the top and bottom panels respectively. On both panels we overplot in yellow the local starburst spectral template of Brandl et al. (2006), the averaged spectrum of the high-redshift sub-millimeter galaxies from Menéndez-Delmestre et al. (2009) in pink, as well as the template of the $z \sim 2$ ULIRGs from Farrah et al. (2008) in cyan. b) Plot of the FEE of the continuum at $13.2 \mu\text{m}$ as a function of the IR luminosity for the galaxies of our sample (blue circles). The size of the circles scales with the distance to the galaxy. The red squares in the left and right panels are the results obtained for a sub-sample of galaxies taken from the starburst sample of Brandl et al. (2006). The size of the squares also scales with distance. For reference, the projected linear size of the unresolved component at the given distance is shown in parenthesis. The background faint (blue) line is a normalized histogram of the galaxies at different IR luminosity bins. The solid (black) line is the median of the $FEE_{13.2\mu\text{m}}$ at the different luminosity bins. The lower and upper dashed lines are the minimum and maximum $FEE_{13.2\mu\text{m}}$ at each bin respectively. The upper limits marked with orange arrows indicate galaxies whose core sizes are unresolved.

resolved. If we consider the ULIRGs located up to a distance of $\sim 100 \text{ Mpc}$ as the reference, we can estimate an upper limit for their core sizes of $\sim 1.5 \text{ kpc}$, which is in agreement with previous findings (e.g., Soifer et al. 2001).

In order to put our results for the GOALS sample in the context of the less luminous but more numerous galaxies of our local universe, we have analyzed the low luminosity sources from the starburst sample of (Brandl et al. 2006). We selected galaxies with $L_{\text{IR}} \leq 10^{11} L_{\odot}$ where the IRS slit was well centered on their nuclei. Our measurements are plotted as red squares in Figure 2b. We find that the $FEE_{13.2\mu\text{m}}$ of these systems ranges between $\sim 0.4 - 0.8$ and is within the values shown by GOALS galaxies with similar IR luminosities. This suggests that the extent of the MIR continuum emission in starburst galaxies and in the low luminosity tail of the GOALS LIRGs is comparable.

2.3. Dependence of Extended Emission on the Stage of Interaction and Presence of An AGN

We have shown that there is a strong evolution of the compactness of the continuum MIR emission at the transition point from LIRGs to ULIRGs. What is the physical process responsible for this? It is known that most ULIRGs are merging systems with clear signs of interactions (e.g., Clements et al. 1996; Murphy et al. 2001). Could it

be that the merging processes in (U)LIRGs which drive the material of the galaxies to their nuclei causing massive star formation, is the same reason that makes them appear more compact in the MIR?

The galaxies of GOALS have been already classified by Petric et al. (2011) in 5 stages: (0) no obvious sign of disturbance in their IRAC or *HST* morphologies, or published evidence that the gas is in dynamical equilibrium (i.e., undisturbed circular orbits); (1) early stage, where the galaxies are within one arc-minute of each other, but little or no morphological disturbance can be observed; (2) the galaxies exhibit bridges, strong disturbance but they do not have a common envelope and each optical disk is relatively intact; (3) the optical disks are completely destroyed but 2 nuclei can be distinguished; (4) the two interacting nuclei are merged but structure in the disk indicates the source has gone through a merger. We observe Díaz-Santos et al. (see also Fig. 5 of 2010b) that the most advanced mergers (stage 4) tend to have low $FEE_{13.2\mu\text{m}}$ values, i.e., they are more compact. K-S tests performed between the total, stage 4 $FEE_{13.2\mu\text{m}}$ distribution and those of the rest of merging stages yield significance values always lower than 0.01. K-S tests performed among the 0 – 3 merging stage datasets provide significance values between 0.4 and 0.75. This implies that in fact galaxies classified as to be at merging stage 4 are systematically more compact.

Another reason why LIRGs and ULIRGs may appear compact in the MIR is the presence of a dominant AGN. We know that the AGN activity is more prevalent in high IR luminosity systems (e.g., Veilleux et al. 1995, 2009), so we would expect that as the AGN emission starts to dominate the IR energy output of a galaxy, it appears progressively less extended.

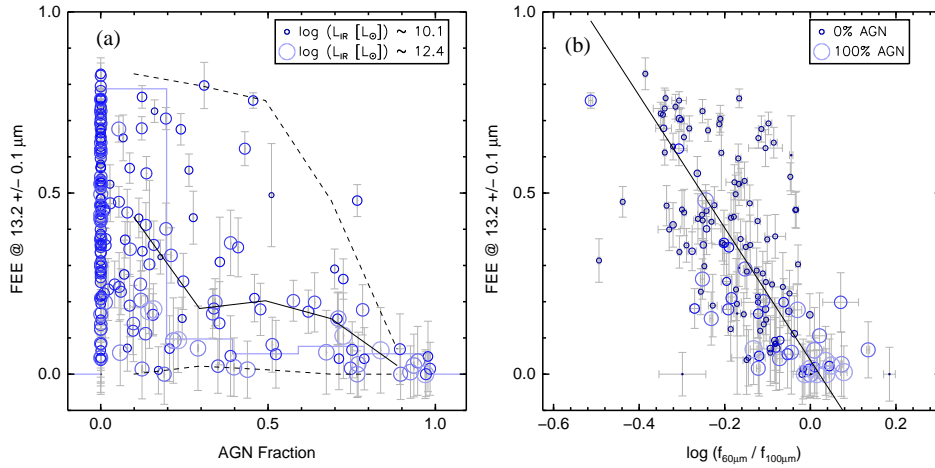


Figure 3. a) FEE of the $13.2\mu\text{m}$ continuum emission as a function of the AGN fraction, estimated by the $6.2\mu\text{m}$ PAH equivalent width, for the galaxies of our sample (see Petric et al. 2011). The size of the circles scales with the L_{IR} of the galaxies. The background faint blue line is the normalized histogram of the AGN fraction. The solid black line is the median of the $FEE_{13.2\mu\text{m}}$ at the different bins of AGN-fraction. The lower and upper dashed lines are the minimum and maximum $FEE_{13.2\mu\text{m}}$ at each bin respectively. b) FEE of the $13.2\mu\text{m}$ continuum emission as a function of the IRAS $\log(f_{60\mu\text{m}}/f_{100\mu\text{m}})$ color. The sizes of the circles scale with the AGN fraction of the galaxies. Points indicate galaxies for which the AGN-fraction was not available. The solid line is the linear fit to the data.

For all galaxies in our sample the contribution of an AGN to their MIR emission has been estimated by Petric et al. (2011) using a number of line and continuum features. We use their estimates of the AGN fraction calculated by means of the so-called ‘‘Laurent diagram’’ (Laurent et al. 2000), which is based on the $15\ \mu\text{m}/5.5\ \mu\text{m}$ continuum and $6.2\ \mu\text{m}\ \text{PAH}/5.5\ \mu\text{m}$ ratios. By comparing the data in this parameter space with representative ratios of pure AGN, PDR, and HII regions, it is possible to infer the contribution of these components to the total galaxy emission. In Figure 3a we present the $FEE_{13.2\ \mu\text{m}}$ as a function of this AGN fraction for the 210 galaxies for which it could be derived. The galaxies are again displayed as circles, the size of which scales with their IR luminosity. It is clear that as the AGN fraction approaches unity, the maximum $FEE_{13.2\ \mu\text{m}}$ at the different AGN-fraction bins (upper dashed line) decreases and the galaxies become progressively more compact. In addition, the median $FEE_{13.2\ \mu\text{m}}$ (solid line) also decreases as the AGN fraction increases, although more smoothly. In fact, only 5 out of the 30 AGN-dominated galaxies² have $FEE_{13.2\ \mu\text{m}} > 0.2$. Independently of the L_{IR} , it is interesting to see that 60% (15/25) of the AGN-dominated galaxies with $FEE_{13.2\ \mu\text{m}} \leq 0.2$ are in the final stage of interaction, while only 12% (3/25) are in the 3rd, 0 in the 2nd, 20% (5/25) in the 1st and 8% (2/25) in the 0th.

We have found that galaxies classified as mergers in their final stage of interaction tend to have low $FEE_{13.2\ \mu\text{m}}$ values and, in particular for ULIRGs, $FEE_{13.2\ \mu\text{m}} < 0.2$. We also show now that the fraction of ULIRGs in merging stage 4 that are AGN-dominated is 60% (9/15). The fraction of galaxies with $10^{11.25}\ L_{\odot} \leq L_{\text{IR}} < 10^{12}\ L_{\odot}$ and $FEE_{13.2\ \mu\text{m}} \leq 0.2$ that are AGN-dominated is 33% (5/15)³ while for lower luminosity systems is 33% (1/3). Moreover, the fraction of AGN-dominated galaxies classified as mergers at stage 4 with $FEE_{13.2\ \mu\text{m}} > 0.2$ is 0%, independently of the IR luminosity. That is, all AGN-dominated galaxies in the stage 4 of interaction are compact.

2.4. Extended Emission and Presence of Cold Dust

Independently of the process that dominates the IR emission in galaxies (either an AGN or a starburst), we should expect to observe harder radiation fields and higher dust temperatures within more compact environments. In this section we explore whether the extended emission we detect in the $5 - 15\ \mu\text{m}$ wavelength range, that traces warm small dust grains and molecules, depends on the amount of cold dust of our sources. We first calculate the *IRAS* $\log(f_{60\ \mu\text{m}}/f_{100\ \mu\text{m}})$ color of the galaxies, which is a well known IR broad-band AGN diagnostic (de Grijp et al. 1985), but we find that it does not correlate with the extent of the MIR continuum emission. We also explore whether there is a dependence on the *Spitzer* $\log(f_{24\ \mu\text{m}}/f_{70\ \mu\text{m}})$ and $\log(f_{70\ \mu\text{m}}/f_{160\ \mu\text{m}})$ colors but do not find any clear trend. However, when we plot in Figure 3b the $FEE_{13.2\ \mu\text{m}}$ as a function of the FIR *IRAS* $\log(f_{60\ \mu\text{m}}/f_{100\ \mu\text{m}})$ color, a correlation is visible. Despite the large scatter, galaxies with cold FIR colors appear to be more extended in their MIR continuum. The Spearman rank correlation coefficient is -0.67 with a significance level of effectively 0, while the Kendall test provides a value of -0.49 , implying that the correlation is real. We fitted our data with an outlier-resistant linear fit algorithm and the best fit parameters are given in the following equation:

²We define as AGN-dominated galaxies those that have an AGN fraction larger than 0.5.

³We have AGN classification for 15 out of 16 galaxies in each of the ULIRG and $10^{11.25}\ L_{\odot} \leq L_{\text{IR}} < 10^{12}\ L_{\odot}$ luminosity bins.

$$FEE_{13.2\mu\text{m}} = 0.04 \pm 0.02 - (1.83 \pm 0.11) \times \log\left(\frac{f_{60\mu\text{m}}}{f_{100\mu\text{m}}}\right) \quad (2)$$

where $FEE_{13.2\mu\text{m}}$ is the fraction of the extended emission of a given galaxy at $13.2\mu\text{m}$, and $f_{60\mu\text{m}}$ and $f_{100\mu\text{m}}$ are the *IRAS* flux densities (f_ν) at 60 and $100\mu\text{m}$, respectively. The data have a scatter of 0.2 in the y-axis and 0.1 in the x-axis. The uncertainties in the parameters of the fit have been calculated using bootstrapping resampling analysis. In order to avoid interacting systems for which only one *IRAS* color has been measured due to the limited spatial resolution, we have used only 142 sources for which there is a unique association between one galaxy (one $FEE_{13.2\mu\text{m}}$ measurement) and one *IRAS* color. In addition to this correlation, Figure 3b also shows that nearly all galaxies whose MIR emission is dominated by an AGN (i.e., they have a high AGN fraction according to the estimates of Petric et al. 2011) are located at the lower right corner of the plot, which means that they are more compact, and have warmer FIR colors. Even if we exclude AGN dominated systems and consider only starburst galaxies with an AGN fraction close to zero, the correlation is still present.

This result has an interesting implication for the forthcoming studies of the cold dust emission of LIRGs/ULIRGs with the *Herschel Space Telescope*. Figure 3b suggests that “cold” FIR-selected (U)LIRGs will likely present large $FEE_{13.2\mu\text{m}}$ values. As a result one would expect that a large fraction of their MIR continuum emission originates in their extended component (see previous section). Furthermore, based on the study by Bothun & Rogers (1992), the *IRAS* $\log(f_{60\mu\text{m}}/f_{100\mu\text{m}})$ colors of our galaxies suggest that they have very strong dust temperature gradients (their Section 4.1 and Table 3). Consequently the cold, FIR emission from these systems will be more extended than the warmer MIR emission. Taking this into account, the FEE we derive for the MIR continuum emission based on our *Spitzer/IRS* observations places a lower limit to the extent of the FIR continuum emission. Therefore, despite the limitations of our long-slit MIR spectra, one may obtain a rough estimate on how much of the FIR emission is extended in any LIRG/ULIRG.

3. Conclusions

Based on the analysis of the spatial profiles of low-resolution $5\text{-}15\mu\text{m}$ *Spitzer/IRS* spectra of the GOALS sample we find that:

- There is a diversity in the shape of the FEE_λ as a function of wavelength. The variation in the spatial extent of the various MIR features such as PAHs, emission lines, and continuum implies that the MIR emission in (U)LIRGs is complex. However, we find 3 types of FEE_λ functions: constant/featureless, PAH-/line-extended, and silicate-extended. Several physical processes, such as AGN emission as well as multiple bursts of star formation, nuclear and extra-nuclear, are suggested to produce the integrated MIR spectrum of (U)LIRGs and to determine their spatial extent at different wavelengths.
- More than 90% of the galaxies in the GOALS sample have median FEE_λ larger than 0.1. Furthermore, more than 30% of the galaxies have median FEE_λ larger than 0.5, implying that at least half of their MIR emission is extended. As a whole, the median FEE_λ of local LIRGs is $\sim 2 - 3$ times larger than that of ULIRGs.

- The spectra (features and continuum emission) of the extended emission component of all (U)LIRGs is very similar, indicating that the properties of the star formation in the external parts (disks) of galaxies ($d \gtrsim 2$ kpc) are the same.
- Despite the limited spatial resolution of the *Spitzer*/IRS spectra, we find a steep decrease in the extent of the continuum emission, $FEE_{13.2\mu\text{m}}$, at the threshold of $L_{\text{IR}} \sim 10^{11.8} L_{\odot}$. While LIRGs display a wide range of $FEE_{13.2\mu\text{m}}$, spanning from compact objects to sources extended up to 85%, galaxies above this threshold show unresolved cores and very compact emission, in particular ULIRGs, which all have $FEE_{13.2\mu\text{m}} \lesssim 0.2$ independently of their distance. We measure galaxy core sizes (FWHMs) of LIRGs at $13.2\mu\text{m}$ up to 10 kpc, with a mean of 2.6 kpc if upper limits to the sizes of unresolved galaxies are taken into account. If only resolved sources are considered, the mean core size of LIRGs is 3.1 kpc. Our estimate for those of ULIRGs is less than 1.5 kpc.
- Galaxies classified as mergers in their final stage of interaction, based on imaging from the *Hubble* and *Spitzer Space Telescopes*, show lower $FEE_{13.2\mu\text{m}}$ values than galaxies in earlier stages. Galaxies with $10^{11.25} L_{\odot} \leq L_{\text{IR}} < 10^{12} L_{\odot}$ in their final stage of interaction also display a similar trend (like ULIRGs), showing lower $FEE_{13.2\mu\text{m}}$ values than less luminous systems.
- The maximum and the median $FEE_{13.2\mu\text{m}}$ decrease as the AGN-fraction increases. Galaxies with AGN-fractions larger than 50% are more compact, and 60% of those that have $FEE_{13.2\mu\text{m}} < 0.2$ are systems in the final stage of interaction. Furthermore, *all* AGN-dominated galaxies classified as mergers in their final stage of interaction have $FEE_{13.2\mu\text{m}} < 0.2$, i.e., are compact, independently of their L_{IR} .
- The $FEE_{13.2\mu\text{m}}$ and the *IRAS* $\log(f_{60\mu\text{m}}/f_{100\mu\text{m}})$ color appear to be correlated, with the MIR continuum emission of colder galaxies being more extended. Due to the large temperature gradients present in our galaxies, the FEE of the MIR continuum provides a rough lower limit to the FEE of the FIR emission in these systems.
- We find no evidence that the local ULIRGs of the GOALS sample are extended in the MIR to the sizes suggested by the $\text{H}\alpha$ or CO measurements of high- z sources. Instead it is the LIRG population that displays resolved emission extended over several kpc scales. In addition, it appears that the SMG population comprises not only isolated, disk-like galaxies but also merging systems, which is also in agreement with our findings for the LIRG class.

Determining the extent of a galaxy at MIR, FIR, and even radio wavelengths can yield information about how the stellar populations are distributed in it, and therefore reveal how the galaxy has formed and evolved. These questions will be soon addressed by new observations obtained with the *Herschel Space Telescope* and the Atacama Large Millimeter Array (ALMA), and in the more distant future with the *James Webb Space Telescope*.

Acknowledgments. The author is grateful to Dr. Lei Hao (Shanghai Observatory) and Dr. Yu Gao (Purple Mountain Observatory) for hosting him in China, and would like to also acknowledge the financial support of the organizers of the Guilin conference for making this visit possible.

References

- Alexander, D. M., Swinbank, A. M., Smail, I., et al. 2010, *MNRAS*, 402, 2211
Armus, L., Charmandaris, V. Bernard-Salas, J., et al., 2007, *ApJ*, 656, 148
Armus, L., et al. 2009, *PASP*, 121, 559
Bothun, G. D., & Rogers, C. 1992, *AJ*, 103, 1484
Bothwell, M. S., et al. 2010, *MNRAS*, 405, 219
Brandl, B. R., et al. 2006, *ApJ*, 653, 1129
Bryant, P. M., & Scoville, N. Z. 1999, *AJ*, 117, 2632
Caputi, K. I., et al. 2007, *ApJ*, 660, 97
Clements, D. L., Sutherland, W. J., McMahon, R. G., & Saunders, W. 1996, *MNRAS*, 279, 477
de Grijp, M. H. K., Miley, G. K., Lub, J., & de Jong, T. 1985, *Nat*, 314, 240
Desai, V., et al. 2007, *ApJ*, 669, 810
Díaz-Santos, T., Alonso-Herrero, A., Colina, et al. 2008, *ApJ*, 685, 211
Díaz-Santos, T., Alonso-Herrero, A., Colina, L., et al. 2010, *ApJ*, 711, 328
Díaz-Santos, T., Charmandaris, V., Armus, L., et al. 2010, *ApJ*, 723, 993
Díaz-Santos, T., Charmandaris, V., Armus, L., et al. 2011, *ApJ*, (submitted)
Downes, D., & Solomon, P. M. 1998, *ApJ*, 507, 615
Farrah, D., et al. 2008, *ApJ*, 677, 957
Fazio, G. G., et al. 2004, *ApJS*, 154, 10
Haan et al., S. 2011, *AJ*, 141, 100
Houck, J. R., et al. 1984, *ApJ*, 278, L63
Houck, J. R., et al. 2004, *ApJS*, 154, 18
Houck, J. R., et al. 2005, *ApJ*, 622, L105
Howell, J. H., et al. 2010, *ApJ*, 715, 572
Imanishi, M., Nakagawa, T., Ohyama, Y., et al. 2008, *PASJ*, 60, 489
Ivion, R. J., Smail, I., Papadopoulos, P. P., et al. 2010, *MNRAS*, 404, 198
Laurent, O., Mirabel, I. F., Charmandaris, V., et al. 2000, *A&A*, 359, 887
Le Floch, E., Charmandaris, V., Laurent, O., et al. 2002, *A&A*, 391, 417
Le Floch, E., et al. 2005, *ApJ*, 632, 169
Menéndez-Delmestre, K., et al. 2009, *ApJ*, 699, 667
Murphy, E. J., Chary, R., Alexander, D. M., et al. 2009, *ApJ*, 698, 1380
Murphy, Jr., T. W., Soifer, B. T., Matthews, K., & Armus, L. 2001, *ApJ*, 559, 201
Pereira-Santaella, M., Alonso-Herrero, A., Rieke, G. H., et al. 2010, *ApJS*, 188, 447
Pérez-González, P. G., et al. 2005, *ApJ*, 630, 82
Petric et al., A. O. 2011, *ApJ*, (in press arXiv:1012.1891)
Pope, A., et al. 2008, *ApJ*, 675, 1171
Rieke, G. H., et al. 2004, *ApJS*, 154, 25
Rigby, J. R., et al. 2008, *ApJ*, 675, 262
Sanders, D. B., & Mirabel, I. F. 1996, *ARA&A*, 34, 749
Sanders, D. B., Mazzarella, J. M., Kim, et al. 2003, *AJ*, 126, 1607
Soifer, B. T., & Neugebauer, G. 1991, *AJ*, 101, 354
Soifer, B. T., et al. 2000, *AJ*, 119, 509
Soifer, B. T., et al. 2001, *AJ*, 122, 1213
Spoon, H. W. W., et al. 2004, *ApJS*, 154, 184
Tacconi, L. J., et al. 2008, *ApJ*, 680, 246
Veilleux, S., Kim, D.-C., Sanders, D. B., Mazzarella, J. M., & Soifer, B. T. 1995, *ApJS*, 98, 171
Veilleux, S., et al. 2009, *ApJS*, 182, 628
Werner, M. W., et al. 2004, *ApJS*, 154, 1
Yan, L., et al. 2005, *ApJ*, 628, 604